Increased Persistent Sodium Current Due to Decreased PI3K Signaling Contributes to QT Prolongation in the Diabetic Heart

Zhongju Lu,[1] Ya-Ping Jiang,[1] Chia-Yen C. Wu,[1] Lisa M. Ballou,[1] Shengnan Liu,[1] Eileen S. Carpenter,[2] Michael R. Rosen,[1,3] Ira S. Cohen,[1] and Richard Z. Lin[1,4]

Diabetes is an independent risk factor for sudden cardiac death and ventricular arrhythmia complications of acute coronary syndrome. Prolongation of the QT interval on the electrocardiogram is also a risk factor for arrhythmias and sudden death, and the increased prevalence of QT prolongation is an independent risk factor for cardiovascular death in diabetic patients. The pathophysiological mechanisms responsible for this lethal complication are poorly understood. Diabetes is associated with a reduction in phosphoinositide 3-kinase (PI3K) signaling, which regulates the action potential duration (APD) of individual myocytes and thus the QT interval by altering multiple ion currents, including the persistent sodium current I_{NaP}. Here, we report a mechanism for diabetes-induced QT prolongation that involves an increase in I_{NaP} caused by defective PI3K signaling. Cardiac myocytes of mice with type 1 or type 2 diabetes exhibited an increase in APD that was reversed by expression of constitutively active PI3K or intracellular infusion of phosphatidylinositol 3,4,5-trisphosphate (PIP3), the second messenger produced by PI3K. The diabetic myocytes also showed an increase in I_{NaP} that was reversed by activated PI3K or PIP3. The increases in APD and I_{NaP} in myocytes translated into QT interval prolongation for both types of diabetic mice. The long QT interval of type 1 diabetic hearts was shortened by insulin treatment ex vivo, and this effect was blocked by a PI3K inhibitor. Treatment of both types of diabetic mouse hearts with an I_{NaP} blocker also shortened the QT interval. These results indicate that downregulation of cardiac PI3K signaling in diabetes prolongs the QT interval at least in part by causing an increase in I_{NaP}. This mechanism may explain why the diabetic population has an increased risk of life-threatening arrhythmias. ***Diabetes* 62:4257–4265, 2013**

Patients with diabetes are at increased risk of developing life-threatening cardiac arrhythmias, independent of other risk factors such as atherosclerosis and hypertension. Diabetes is an independent risk factor for sudden cardiac death, mortality after myocardial infarction, and major complications of acute coronary syndrome such as ventricular arrhythmias (1). However, pathophysiological mechanisms responsible for the increased risk of sudden cardiac death remain poorly understood, and consequently there has been relatively little progress in the prevention and treatment of this diabetes complication. QT interval prolongation on the electrocardiogram (ECG) is a well-established risk factor for lethal ventricular arrhythmias (2), and not only do diabetic patients have a greater prevalence of QT interval prolongation than control populations (3,4), but a prolonged QT interval corrected for heart rate (QTc) is an independent risk factor for cardiovascular death in diabetic people (5–7).

The signaling defect that causes QT interval prolongation in diabetes has remained elusive. An interesting lead came from our recent demonstration that decreased cardiac phosphoinositide 3-kinase (PI3K) signaling results in QT interval prolongation and is responsible for the increased risk of long QT syndrome and lethal arrhythmias caused by some anticancer drugs (8). Our results raised the possibility that suppression of this signaling pathway might also play a role in QT interval prolongation associated with diabetes, where reduced production of or sensitivity to insulin results in decreased activation of PI3K and its downstream effector, Akt.

Primary prolongation of the QT interval (i.e., that which is independent of an altered QRS complex on the ECG) results from lengthening of the action potential duration (APD) in individual cardiac myocytes. The APD is regulated by inward and outward ion currents, and our previous study demonstrated that PI3K signaling regulates both types. PI3K inhibition caused reductions in the L-type calcium current (I_{CaL}), the delayed rectifier potassium currents I_{Kr} and I_{Ks}, and the peak sodium current (I_{Na}), whereas it caused an increase in the persistent (late) sodium current (I_{NaP}) (8). In the current study, we used mouse models to investigate a possible connection between decreased cardiac PI3K signaling and the prolonged QT interval in diabetes. Whereas I_{Kr} and I_{Ks} play little or no role in regulating the APD in adult mouse myocytes (9,10), I_{NaP} has a major role, such that expression of gain-of-function mutant sodium channels that increase I_{NaP} prolongs the murine APD and QT interval (11,12). Therefore, we used I_{NaP} as a marker of PI3K effects on cardiac ion channels and asked whether an increase in I_{NaP} contributes to QT interval prolongation in these diabetic mouse models.

RESEARCH DESIGN AND METHODS

Animals. Insulin-deficient C57BL/6-*Ins2*^{Akita}/J (*Ins2*^{Akita}) and insulin-resistant B6.BKS(D)-*Lepr*^{db}/J (*db/db*) mice in the C57BL/6J background were purchased from Jackson Laboratory (Bar Harbor, ME). For both groups, control animals were wild-type C57BL/6J mice. Animals were analyzed between 2 and 3

From the [1]Department of Physiology and Biophysics and the Institute for Molecular Cardiology, Stony Brook University, Stony Brook, New York; the [2]Department of Pharmacological Sciences, Stony Brook University, Stony Brook, New York; the [3]Department of Pharmacology, Columbia University, New York, New York; and the [4]Medical Service, Northport VA Medical Center, Northport, New York.

Corresponding author: Ira S. Cohen, ira.cohen@stonybrook.edu, or Richard Z. Lin, richard.lin@stonybrook.edu.

Received 15 March 2013 and accepted 15 August 2013.

DOI: 10.2337/db13-0420

This article contains Supplementary Data online at http://diabetes.diabetesjournals.org/lookup/suppl/doi:10.2337/db13-0420/-/DC1.

months of age. Hyperglycemia (>500 mg/dL) was confirmed in *Ins2*^{Akita} and *db/db* mice by tail vein blood glucose measurements using a OneTouch UltraMini glucometer (LifeScan, Milpitas, CA). All animal-related experimental protocols were approved by the Stony Brook University Institutional Animal Care and Use Committee and conform to National Institutes of Health (NIH) standards.

Ventricular myocyte isolation and primary culture. Mouse ventricular myocytes were isolated from mice fed ad libitum as previously described (8). To make myocyte cultures, hearts harvested from adult mice were first perfused with Ca^{2+}-free myocyte buffer (137 mmol/L NaCl, 5.4 mmol/L KCl, 2 mmol/L $MgSO_4$, 0.33 mmol/L NaH_2PO_4, 10 mmol/L HEPES, 10 mmol/L taurine, 10 mmol/L glucose, and penicillin-streptomycin, pH 7.4) followed by digestion with Liberase TH (Roche) and 0.1 mmol/L Ca^{2+} in myocyte buffer. Digestion was stopped by perfusion with myocyte buffer containing 0.2 mmol/L Ca^{2+} and 1% BSA. The tissue was dissociated by mechanical force, and isolated cells were filtered through 210-μm nylon mesh to remove debris. Settled myocytes were then washed with myocyte buffer containing 1% BSA with increasing concentrations of Ca^{2+} up to 1.0 mmol/L. Viable myocytes were resuspended in culture medium (medium 199 supplemented with 2 mmol/L carnitine, 5 mmol/L creatine, 5 mmol/L taurine, 0.2% BSA, 100 units/mL penicillin, 100 μg/mL streptomycin, 1.75 μmol/L bovine insulin, 5.5 μg/mL transferrin, 6.7 ng/mL selenium, and 25 μmol/L blebbistatin with physiological levels of Ca^{2+}) with 5% FBS and cultured on laminin-coated dishes at 37°C with a 5% CO_2 atmosphere for 2 h and then changed to serum-free culture medium for another 4 h prior to adding adenoviruses. The next day, cell culture medium was changed to contain either 1 nmol/L bovine insulin (wild-type and *db/db*) or no insulin (*Ins2*^{Akita}). Electrophysiological or biochemical analyses were performed 24 h later.

Adenoviral PI3K p110α H1047R (CAp110α). Site-directed mutagenesis was used to generate hemagglutinin (HA) epitope–tagged p110α H1047R from wild-type mouse p110α cDNA. Recombinant adenoviruses carrying p110α H1047R were constructed using a method similar to the one described by He et al. (13). In brief, HA-tagged p110α H1047R was cloned into the pAdTrack-CMV shuttle vector using the *Xba*I and *Kpn*I restriction sites. The resulting plasmid was linearized and then electroporated into *BJ*-5183-Ad1 cells (Stratagene). Bacterial colonies were screened for appropriate recombination. The resulting plasmid was linearized with *Pac*I and transfected into HEK293 cells for viral production. Viruses were collected and purified by centrifugation in cesium chloride. Green fluorescent protein (GFP)-expressing control adenoviruses were produced using a similar method (14).

Electrophysiology. Recordings were made at room temperature. Only relaxed quiescent cells displaying clear cross striations were used. Standard whole-cell patch-clamp techniques were performed with an Axopatch-1D amplifier with a CV-4 1/100 headstage (Axon Instruments). A personal computer equipped with 12-bit AD/DA converters (model 1360; Cambridge Electronic Design) was used for data acquisition, generation of pulse protocols, and data analysis. Currents were sampled at 10 kHz and filtered with a four-pole Bessel filter at 2 kHz. Current amplitude was normalized to cell capacitance to obtain current density in picoamp/picofarad (pA/pF). In some experiments, 1 μmol/L phospholipids (all di-C8; Echelon Biosciences) were added to the pipette solution. Mexiletine hydrochloride (Sigma-Aldrich) was added to cells for 2 h at room temperature prior to or acutely perfused during patch clamping as indicated. Wild-type myocytes were incubated with Akt inhibitor (Akti) VIII (EMD Millipore) for 2 h prior to patch clamping.

Recording of action potentials in mouse myocytes was initiated in current clamp mode by applying pulses 120 pA in amplitude and 10 ms in duration with a cycle length of 1 s as previously described (8). 4-Aminopyridine (4-AP, 4 mmol/L; Sigma-Aldrich) was added to the external solution to block most of the transient outward current (I_{to}).

The tetrodotoxin (TTX)-sensitive Na^+ current was elicited by 750-ms depolarizing voltage steps ranging from −80 to 0 mV at 10-mV increments from a holding potential of −80 mV. The pipette solution contained 111 mmol/L CsCl, 20 mmol/L tetraethylammonium chloride, 14 mmol/L EGTA, 5 mmol/L MgATP, 10 mmol/L HEPES, and 10 mmol/L glucose. The pH of the pipette solution was adjusted to 7.4 with 39 mmol/L CsOH. The external solution contained 90 mmol/L CsCl, 1.2 mmol/L $MgCl_2$, 1 mmol/L $CaCl_2$, 10 mmol/L tetraethylammonium chloride, 5 mmol/L HEPES, 11 mmol/L glucose, and 50 mmol/L NaCl. The pH of the external solution was adjusted to 7.4 with CsOH. I_{NaP} was measured as the main inward current between 700 and 750 ms at the end of depolarization. TTX-sensitive currents were measured by subtracting a trace obtained in the presence of 10 μmol/L TTX from a trace obtained in its absence. I_{NaP} records were filtered at 20 Hz. For the single trace of TTX-sensitive current shown in the figures, the current was activated at a test voltage of −20 mV from a holding potential of −80 mV.

Recording of cardiac electrical activity ex vivo. Isolated mouse hearts were mounted on the IH-SR isolated heart perfusion system (Harvard Apparatus) and perfused with Krebs-Henseleit solution (118 mmol/L NaCl, 4.7 mmol/L KCl, 2.52 mmol/L $CaCl_2$, 1.64 mmol/L $MgSO_4$, 24.88 mmol/L $NaHCO_3$, 1.18 mmol/L KH_2PO_4, 5.55 mmol/L glucose, and 2 mmol/L sodium pyruvate aerated with 5% CO_2 and 95% O_2) at 37°C for 30 min to reach a stable baseline prior to data collection. For electrocardiographic recording, one electrode was placed at the base of the heart next to the left atrium, and a second electrode was placed at the heart apex held by pressure. Recordings were collected under control conditions, and then human insulin (Novolin R; Novo Nordisk), PI-103 (Cayman Chemical), or mexiletine was added to the perfusate reservoir and circulated through the system for 30 min prior to collecting another set of recordings. QT intervals were measured automatically by the LabChart 7.1.2 (ADInstruments) software system from >30 consecutive heart beats, and QTc was calculated using the correction described by Mitchell et al. (15) or by Bazett's formula.

Insulin signaling. Mice were fasted overnight. Harvested hearts were perfused with Krebs-Henseleit solution as described above, and then either normal saline or human insulin (1 unit/L) was added to the perfusate reservoir and circulated through the hearts for 10 min. The left ventricles were collected and stored in liquid nitrogen. For PI3K assays, pieces of tissue were homogenized in RIPA buffer containing 50 mmol/L HEPES, pH 7.5, 10 mmol/L sodium pyrophosphate, 50 mmol/L NaCl, 50 mmol/L NaF, 5 mmol/L EDTA, 1 mmol/L sodium orthovanadate, 0.25% sodium deoxycholate, 1% NP-40, 0.2 mmol/L phenylmethylsulfonyl fluoride, and 2 μL/mL protease inhibitor cocktail (Sigma-Aldrich). After centrifugation, aliquots of supernatant containing equal amounts of protein (Bradford assay; Bio-Rad) were mixed with antiphosphotyrosine antibody 4G10 coupled to agarose (Millipore) for 3 h at 4°C. After washing the beads several times with RIPA buffer and then with PI3K assay buffer (20 mmol/L HEPES, pH 7.4, 100 mmol/L NaCl, and 0.5 mmol/L EGTA), they were resuspended in 40 μL PI3K assay buffer. Assays were started by adding L-α-phosphatidylinositol (Sigma-Aldrich) and a reaction mix containing [γ-^{32}P]ATP (PerkinElmer Life Sciences), and the reactions were carried out and processed as previously described (16). After thin-layer chromatography, radioactive spots containing phosphatidylinositol phosphate were visualized by autoradiography, cut out of the plate, and quantified by scintillation counting.

Western blotting. For Akt phosphorylation, Western blotting was performed on the heart lysates as previously described (17) using antibodies to phospho-T473 Akt (Cell Signaling) and total Akt (Santa Cruz Biotechnology). PDK1 and PTEN antibodies were purchased from Cell Signaling; Nav1.5 antibodies were from Alomone Laboratories or EMD Millipore. The bands visualized on film were quantified by NIH ImageJ software. Bands visualized by ProteinSimple FluorChem E (Santa Clara, CA) were quantified by software provided by the company.

RESULTS

Freshly isolated ventricular myocytes from hyperglycemic (>500 mg/dL) insulin-deficient *Ins2*^{Akita} and insulin-resistant *db/db* mice were studied in patch-clamp experiments to determine the APD at 90% repolarization (APD_{90}). As in our previous study (8), we performed our action potential recording in the presence of 4-AP to eliminate most of the large transient outward current I_{to} to produce a longer action potential that allowed us to more easily determine the effects on APD, which might be more relevant to larger mammals. Representative action potentials recorded from *Ins2*^{Akita}, *db/db*, and wild-type myocytes are shown in Fig. 1*A*–*C*. APD_{90} in both types of diabetic myocytes was markedly longer than in wild-type cells (Fig. 1*D*). When phosphatidylinositol 3,4,5-trisphosphate (PIP3), the second messenger produced by PI3K, was added to the patch pipette to dialyze the cell interior, APD_{90} of *Ins2*^{Akita} and *db/db* myocytes decreased to near wild-type levels (Fig. 1*A* and *D*). In contrast, addition of the control phospholipids phosphatidylinositol 4,5-bisphosphate [PI(4,5)P2] or phosphatidylinositol 3,5-bisphosphate [PI(3,5)P2] had no effect on APD_{90} (Fig. 1*D*). To test if the long APD of diabetic myocytes is associated with increased I_{NaP}, we incubated the cells for 2 h with the I_{NaP} blocker mexiletine. This drug treatment shortened APD_{90} in both *Ins2*^{Akita} and *db/db* myocytes to wild-type levels (Fig. 1*B* and *D*). Acute perfusion of *Ins2*^{Akita} myocytes with mexiletine had a similar shortening effect on the APD (Supplementary Fig. 1).

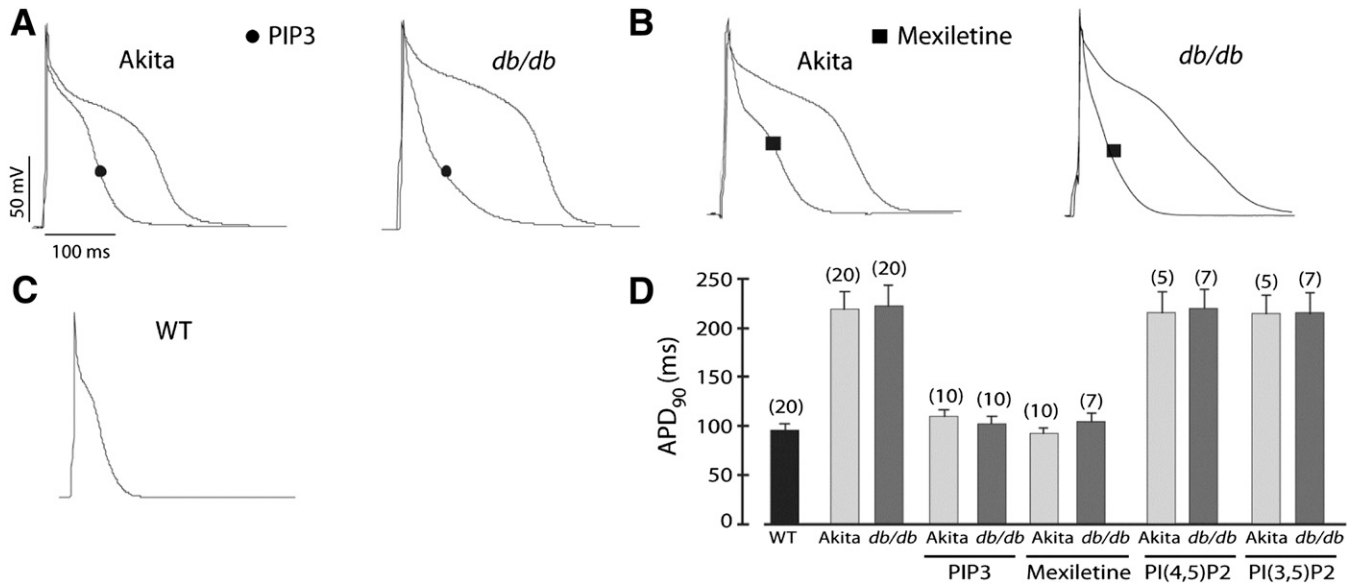

FIG. 1. APD prolongation in diabetic cardiac myocytes and reversal by PIP3 infusion or mexiletine treatment. Ventricular myocytes were prepared from diabetic *Ins2*^{Akita} (Akita) and *db/db* mice. *A*: Sample traces of action potentials with or without intracellular infusion of 1 μmol/L PIP3. *B*: Sample traces of action potentials in myocytes preincubated with 4 μg/mL mexiletine for 2 h. *C*: Sample trace of an action potential in a nondiabetic wild-type (WT) myocyte. *D*: Summary data of APD_{90}. Phospholipids were infused intracellularly at 1 μmol/L. Data shown are mean ± SE. The number of cells studied is above each bar. All studies were performed in the presence of 4-AP.

When action potentials were recorded in the absence of 4-AP, PIP3 and mexiletine still reversed APD prolongation in the diabetic myocytes, but the effect was partial (Supplementary Fig. 2).

The results with mexiletine suggested that APD lengthening in diabetic cardiac myocytes might be due to an increase in I_{NaP}. This was validated in patch-clamp experiments showing an approximately twofold increase in I_{NaP} current density in both *Ins2*^{Akita} and *db/db* myocytes as compared with wild-type cells (Fig. 2*A*). This enhancement in current was present across the entire range of voltages tested (Fig. 2*B*), as was seen in our previous study (8). Infusion of both diabetic cell types with PIP3 caused a reduction in I_{NaP} to wild-type levels (Fig. 2). We saw no consistent change in expression of the Nav1.5 sodium channel that conducts I_{NaP} in the diabetic mouse hearts (Supplementary Fig. 3*A*). Therefore, the increase in I_{NaP} associated with diabetes might be due to alterations in trafficking, gating properties, and/or single channel conductance.

To determine if the increases in APD and I_{NaP} in the diabetic hearts translate into prolongation of the QT interval, we analyzed recordings of electrical activity of Langendorff-perfused hearts. QTc in *Ins2*^{Akita} hearts was increased more than twofold as compared with nondiabetic wild-type hearts (Fig. 3*A* and Supplementary Fig. 4). Furthermore, mexiletine treatment reversed the QTc prolongation, emphasizing the importance of increased I_{NaP} in lengthening the QT interval in this mouse model (Fig. 3*A* and Supplementary Fig. 4). Insulin treatment corrected the abnormal QTc of *Ins2*^{Akita} hearts, and treatment with PI-103, a PI3K inhibitor, blocked the insulin effect (Fig. 3*A* and Supplementary Fig. 4).

Like the *Ins2*^{Akita} hearts, QTc in *db/db* hearts was lengthened more than twofold in comparison with control hearts (Fig. 3*B* and Supplementary Fig. 4). Treatment with mexiletine also shortened the QT interval in this diabetic mouse model, but the effect was only partial (Fig. 3*B* and Supplementary Fig. 4).

We showed in a previous study that PI3K signaling to the protein kinase Akt is downregulated in the heart of *Ins2*^{Akita} mice as compared with nondiabetic wild-type mice, but activation of PI3K/Akt by exogenous insulin is intact (18). Because *db/db* mice develop hyperglycemia despite hyperinsulinemia at a young age, we next investigated if basal and insulin-activated PI3K/Akt signaling are altered in the *db/db* hearts. Spontaneously beating hearts from wild-type and *db/db* mice were mounted on the Langendorff apparatus and perfused with insulin or vehicle for 10 min. Heart lysates were then assayed for PI3K activity or analyzed for Akt phosphorylation by Western blotting. Basal PI3K activity tended to be lower in the *db/db* samples than in wild-type samples (Fig. 4*A*), whereas basal Akt phosphorylation was clearly reduced in *db/db* versus wild-type hearts (Fig. 4*B*). Insulin stimulated a robust increase in PI3K activity (Fig. 4*A*) and Akt phosphorylation (Fig. 4*B*) in the wild-type hearts. In contrast, insulin activation of PI3K and Akt was reduced by 35–40% in the *db/db* hearts as compared with wild-type (Fig. 4). Decreased Akt activation in the two diabetic mouse models does not appear to be due to changes in cardiac expression levels of PTEN or PDK1 (Supplementary Fig. 3*B*). Thus, *db/db* mice exhibit cardiac insulin resistance with respect to PI3K signaling, which we believe leads to QT interval prolongation.

We previously showed that genetic ablation of the PI3K p110α catalytic subunit in cardiac myocytes caused APD prolongation due at least in part to an increase in I_{NaP}, demonstrating the importance of this PI3K isoform in regulating the mouse cardiac action potential (8). Therefore, we assessed whether expression of the constitutively active p110α H1047R mutant (CAp110α) in *db/db* and *Ins2*^{Akita} myocytes shortens the APD. Primary cultures of ventricular myocytes isolated from *db/db* and *Ins2*^{Akita} mice were infected with adenoviruses carrying either CAp110α or GFP as a control. As expected, expression of CAp110α increased Akt phosphorylation (Supplementary

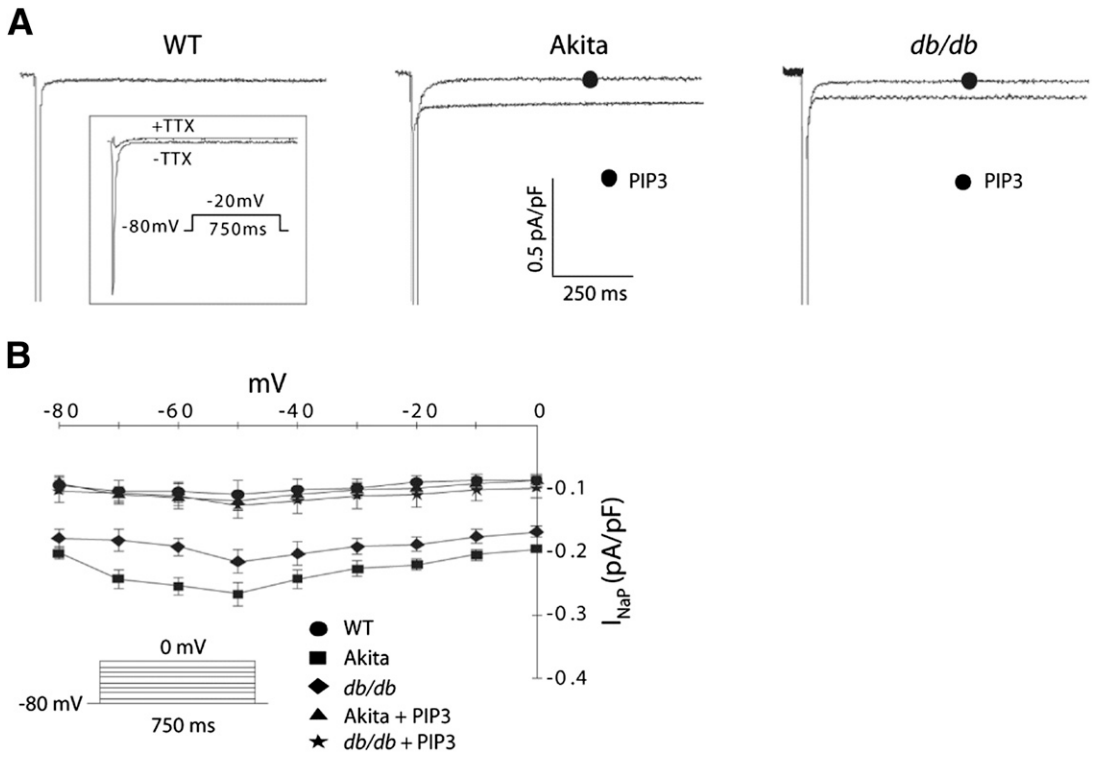

FIG. 2. Increased I_{NaP} in diabetic cardiac myocytes and reversal by PIP3 infusion. *A*: Sample traces of TTX-sensitive I_{NaP} in wild-type (WT), *Ins2*^{Akita} (Akita), and *db/db* myocytes with or without intracellular infusion of 1 μmol/L PIP3. TTX-sensitive currents were obtained by subtracting traces obtained in the presence of 10 μmol/L TTX from the traces obtained in its absence (inset). *B*: Summary graph of I_{NaP}-V relationships shows mean ± SE. I_{NaP} was elicited by depolarizing pulses ranging from −80 to 0 mV in 10-mV increments from a holding potential of −80 mV. *n* = 7 cells for each group.

Fig. 5). Patch-clamp measurements performed in the presence (Fig. 5*A* and *B*) or absence (Supplementary Fig. 6) of 4-AP showed that APD_{90} in *db/db* and *Ins2*^{Akita} myocytes expressing CAp110α was dramatically shortened as compared with the same batch of myocytes infected with adenoviral GFP. Expression of adenoviral CAp110α in cultured wild-type myocytes did not cause a change in APD_{90} as compared with the GFP control (Fig. 5*A* and *B*). It was interesting that APD_{90} in GFP-infected wild-type myocytes was still shorter than in GFP-infected diabetic cells after 2 days in culture (Fig. 5*B*).

Expression of adenoviral CAp110α in cultured *db/db* and *Ins2*^{Akita} myocytes also caused a marked decrease in I_{NaP} (Fig. 5*C–F*). As with the effect of PIP3 on freshly isolated myocytes shown in Fig. 2, the effect of CAp110α on I_{NaP} was evident at all voltages studied. Furthermore, the current density of I_{NaP} in cultured *db/db* and *Ins2*^{Akita} myocytes infected with GFP was similar to the level observed in freshly isolated diabetic myocytes (compare Fig. 2*B* and Fig. 5*E* and *F*), whereas the current density in diabetic myocytes expressing CAp110α was similar to the values for wild-type and diabetic myocytes infused with PIP3 (compare Fig. 2*B* and Fig. 5*E* and *F*). These results indicate that the cultured myocytes retain some of the properties of freshly isolated myocytes and suggest that PI3K is responsible for the regulation of I_{NaP}.

In a converse experiment, we tested whether inhibition of Akt activity in nondiabetic myocytes increases I_{NaP}. Myocytes freshly isolated from wild-type mice were incubated with an Akti prior to patch clamping. We found that this treatment indeed caused an increase in I_{NaP}, but not to the levels seen in myocytes from diabetic mice (Supplementary Fig. 7).

DISCUSSION

The major finding in this study is that an increase in the inward sodium current I_{NaP} plays an important role in causing long QT syndrome in murine models of diabetes. Previous studies suggested that the cardiac repolarization defect in diabetes is due mainly to a decrease in outward potassium currents. Using streptozotocin-induced diabetic rats as a model of type 1 diabetes, it was concluded that APD prolongation is due to reductions in the 4-AP–sensitive transient outward current I_{to} and a 4-AP–insensitive steady-state current referred to as I_K (19–21). A decrease in the inward L-type calcium current I_{CaL} was also seen in streptozotocin-induced diabetic rats (21) and *Ins2*^{Akita} mice (18), but this would tend to shorten the APD. APD prolongation and suppression of outward potassium currents and I_{CaL} were also seen in cardiac myocytes from type 2 diabetic *db/db* mice (22–25). The affected potassium currents in *db/db* mice were not extensively characterized, but were probably equivalent to I_{to} and I_K in the rat studies described above. In comparison with rodents, the magnitude of I_{to} is small in humans and other large mammals. Instead of I_{to}, the outward delayed rectifier potassium currents I_{Ks} and I_{Kr} play a prominent role in regulating cardiac repolarization in large mammals, and some reports demonstrated that these currents can also be altered in diabetes. For example, alloxan-induced diabetic rabbits (a model of type 1 diabetes) exhibited QTc prolongation and reductions in current density of I_{Kr}, I_{Ks}, I_{to}, and I_{CaL}, with no change in peak sodium current (26,27). Computer modeling of the rabbit ventricular action potential suggested that the decrease in I_{Kr} was the major ionic mechanism for diabetic QT prolongation in this model (26). By

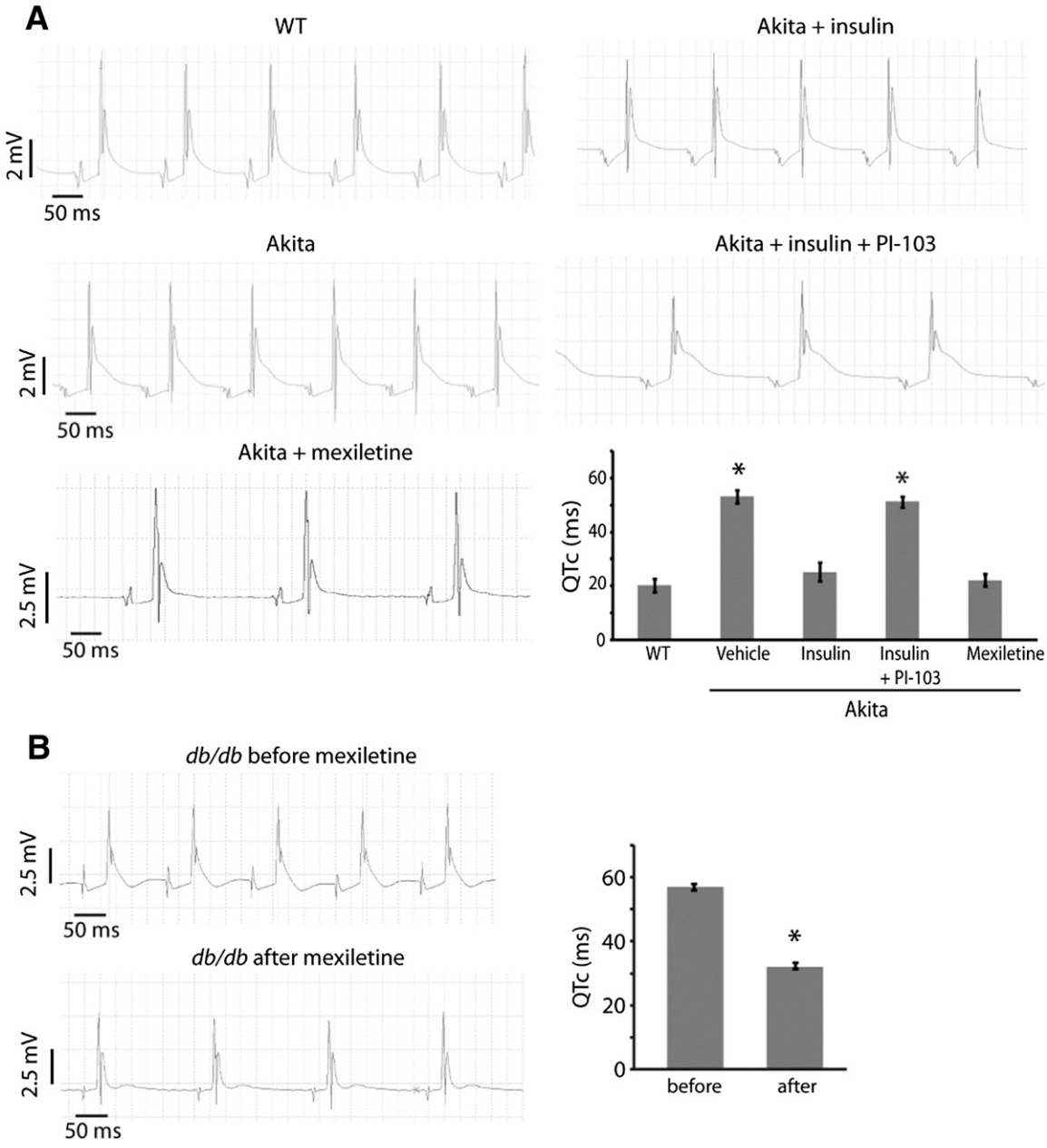

FIG. 3. QT prolongation of *Ins2*^{Akita} (Akita) and *db/db* hearts and reversal by mexiletine. Cardiac electrical activity was recorded from spontaneously beating hearts mounted on a Langendorff apparatus. QT intervals corrected for heart rate (QTc) were automatically calculated from the tracings using the Mitchell formula (15). *A*: Representative tracings from Akita and wild-type (WT) hearts. Hearts were treated with insulin (1 unit/L), PI-103 (500 nmol/L), or mexiletine (4 μg/mL) added to the perfusate. Summary QTc graph shows mean ± SE (*bottom right*). $n \geq 4$ hearts per group. *, significantly different from WT values ($P < 0.05$, ANOVA with post hoc Fisher least significant differences test). *B*: Representative tracings from a *db/db* heart before and after mexiletine treatment. Summary QTc graph shows mean ± SE (*right*). $n = 5$ hearts. *, significantly different from before values ($P < 0.05$, Student *t* test).

contrast, no differences I_{Kr}, I_{CaL}, or the inward rectifier potassium current I_{K1} were seen in cardiac tissue from alloxan-induced diabetic dogs as compared with controls, whereas the current densities of I_{Ks} and I_{to} were significantly lower (28).

To our knowledge, this is the first report in which I_{NaP} was examined in diabetic hearts. We found that I_{NaP} current density was higher in myocytes from *Ins2*^{Akita} and *db/db* mice as compared with wild-type myocytes. Furthermore, treatment of diabetic myocytes with a sodium channel blocker at concentrations somewhat selective for I_{NaP} reduced APD_{90}. In the presence of the I_{to} blocker 4-AP, alterations in I_{to} or other 4-AP–sensitive currents did not contribute to the differences in APD that were observed in control versus diabetic cells. Therefore, it is perhaps not surprising that inhibition of I_{NaP} with mexiletine was sufficient to normalize APD in the diabetic cells under these conditions. The effect of mexiletine was reduced in the absence of 4-AP, indicating that a decrease in I_{to} and other 4-AP–sensitive currents plays a role in determining APD_{90} in the diabetic myocytes. On the other hand, perfusion of *Ins2*^{Akita} hearts with mexiletine resulted in complete normalization of QTc even in the absence of 4-AP. The action potential studies and the ECG studies occur at different

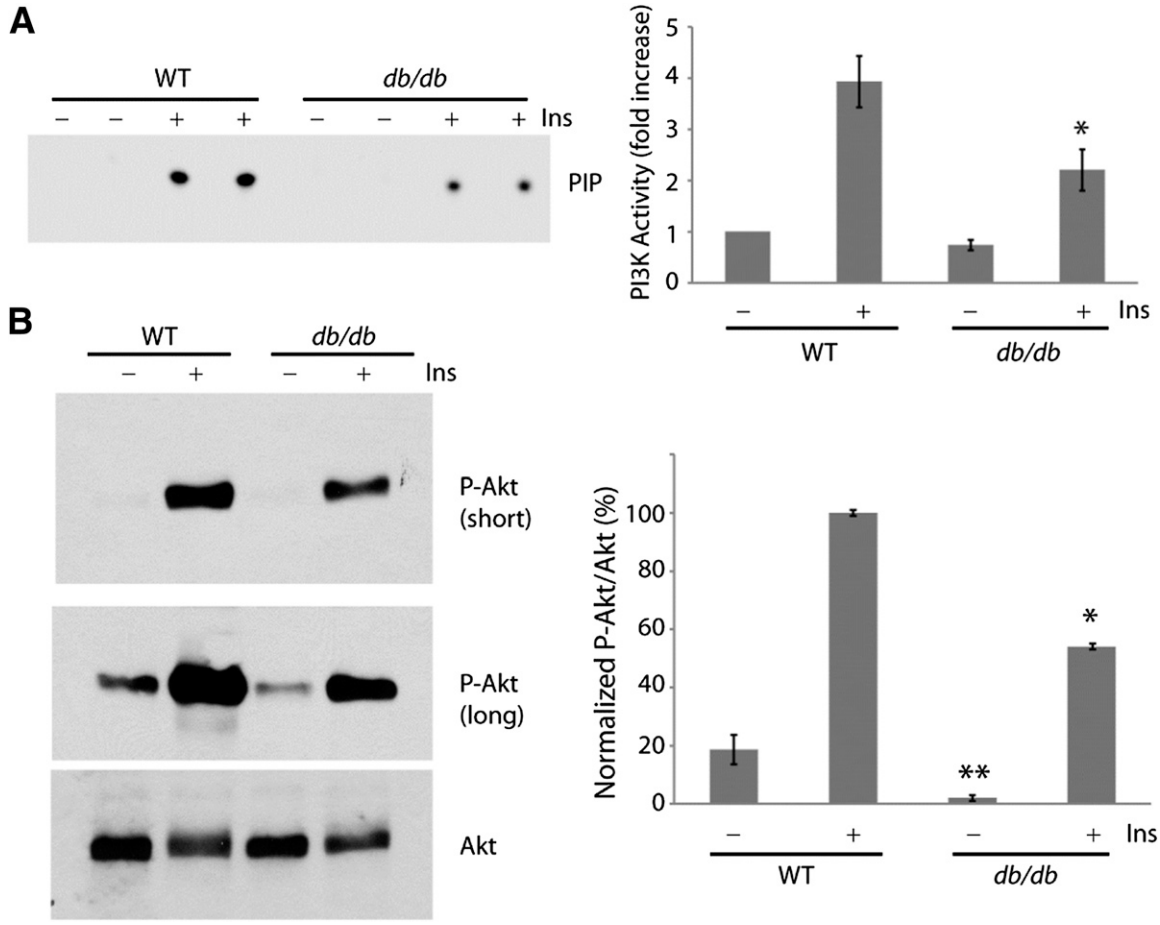

FIG. 4. Attenuated insulin/PI3K/Akt signaling in *db/db* hearts. Wild-type (WT) and *db/db* hearts were perfused with or without 1 unit/L insulin for 10 min while mounted on the Langendorff apparatus. *A*: Representative autoradiograph of PI3K activity (duplicate measurements) assayed in phosphotyrosine immunoprecipitates of heart lysates (*left*). Summary graph of normalized PI3K activity (mean ± SE) from three independent experiments (*right*). *, significantly different from WT treated with insulin ($P < 0.05$, Student t test). *B*: Representative Western blots of heart lysates probed sequentially with phospho-Akt (p-Akt) and total Akt antibodies (*left*). Summary graph of normalized Akt phosphorylation (mean ± SE) from three independent experiments (*right*). *, significantly different from WT treated with insulin; **, significantly different from untreated WT ($P < 0.05$, Student t test). Ins, insulin.

stimulation/heart rates and so the effects on APD and ECG are not simply comparable. However, taking the APD and ECG results together suggests that the increase in I_{NaP} is, at a minimum, a significant contributor to QT interval lengthening in the *Ins2*^{Akita} mouse. Although mexiletine also significantly decreased QTc in *db/db* hearts, the effect was partial. It is possible that QT prolongation in *db/db* hearts is due to an increase in I_{NaP} as well as a decrease in outward potassium currents such as I_{to} and I_K (22).

Patients with type 3 congenital long QT syndrome (LQT3) have gain-of-function mutations in the Nav1.5 sodium channel protein (encoded by *SCN5A*) that cause an increase in I_{NaP} (2). Transgenic mice that express *SCN5A* mutants exhibit many of the phenotypes of LQT3 patients, including elevated I_{NaP}, QT interval prolongation, and cardiac arrhythmias (11,29,30). Mexiletine treatment shortened APD in mouse myocytes expressing an *SCN5A* mutant (29), and it also shortened QTc in LQT3 patients (31). Although mouse models of altered I_{NaP} function have been informative with regard to human LQT3, it is not yet known whether I_{NaP} is increased in diabetic patients. Further studies using cardiac myocytes from diabetic humans or large animal models need to be performed to answer this question and to determine the feasibility of using a sodium channel blocker as a therapy to reduce QT prolongation in diabetes.

The central role of insulin signaling in maintaining normal cardiac electrophysiology was demonstrated in cardiac myocyte–specific insulin receptor knockout mice. Cardiac myocytes from these nondiabetic animals exhibited significant APD prolongation and reduced outward potassium currents (24). Our results provide the following evidence suggesting that low insulin/PI3K signaling is the cause of the cardiac repolarization defect in the diabetic mice studied here. First, intracellular delivery of PIP3, the second messenger produced by PI3K, shortened APD and reduced I_{NaP} in freshly isolated diabetic myocytes. Second, the same effects were produced in cultured diabetic myocytes upon expression of CAp110α. Interestingly, CAp110α did not cause a change in APD_{90} in wild-type cells. Myocytes from transgenic mice with cardiac-specific expression of a different form of constitutively active p110α were also reported to exhibit no significant differences in action potential waveform or ECG parameters as compared with controls (32). Third, perfusion of *Ins2*^{Akita} hearts with insulin caused QTc to shorten, an effect that was blocked by a PI3K inhibitor. We showed earlier that Akt activity is low in *Ins2*^{Akita} hearts as compared

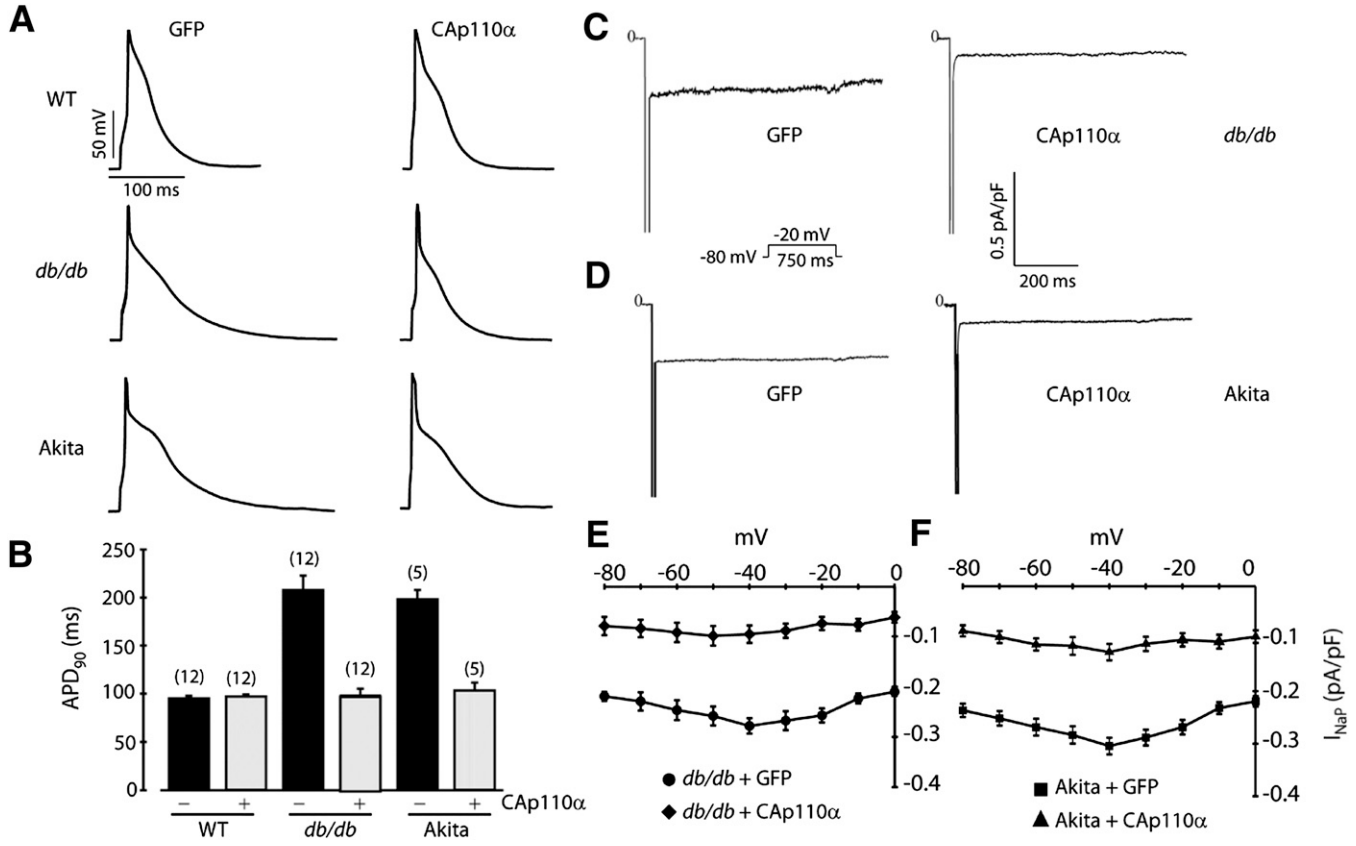

FIG. 5. Expression of constitutively active p110α (CAp110α) reduces APD and I_{NaP} in diabetic myocytes. Cultured myocytes from wild-type (WT), *db/db*, and *Ins2*^{Akita} (Akita) mice were infected with adenoviruses carrying either CAp110α or GFP as a control. *A*: Representative action potential recordings in the presence of 4-AP. *B*: Summary graph of APD_{90} (mean ± SE). The number of cells studied is above each bar. *C*: Representative I_{NaP} tracings recorded in *db/db* myocytes infected with GFP or CAp110α. *D*: Representative I_{NaP} tracings recorded in Akita myocytes infected with GFP or CAp110α. *E*: Summary I_{NaP}-V relationships from *db/db* myocytes. *n* = 8 cells in each group. *F*: Summary I_{NaP}-V relationships from Akita myocytes. *n* = 5 cells in each group.

with nondiabetic hearts, and insulin injection strongly activated cardiac Akt in this diabetic mouse model (18). The ability of insulin to rapidly correct QTc suggests that expression of ion channel proteins that regulate the cardiac action potential (especially Nav1.5) is not greatly altered in *Ins2*^{Akita} hearts, in contrast to what has been observed in some other animal models of diabetes (23,26,28).

A recent report showed that insulin/PI3K/Akt signaling in left ventricular biopsies was increased in diabetic subjects as compared with control subjects (33), suggesting that PI3K/Akt activity is enhanced in the type 2 diabetic heart due to hyperinsulinemia, rather than reduced as a consequence of insulin resistance. On the other hand, Akt phosphorylation in right atrial appendage biopsies tended to be lower in diabetic patients than in control subjects (34). Limitations of these two studies are the small number of subjects involved, cardiovascular disease in the control patients, and the different medications being taken by the control and diabetic groups that could affect the results. In addition, only basal (i.e., fasted) signaling was studied. We show here that insulin activation of PI3K/Akt is blunted in the *db/db* heart. Other investigators have also noted a tendency toward decreased insulin-induced PI3K/Akt activation in cardiac preparations from *db/db* mice (35,36). Attenuated insulin activation of cardiac PI3K/Akt was also reported in *ob/ob* type 2 diabetic mice (33,37) and a porcine model of diet-induced obesity and insulin resistance (38).

The molecular mechanisms involved in insulin/PI3K regulation of I_{NaP} are unknown. A number of protein kinases, including cAMP-dependent protein kinase, protein kinase C, and calmodulin-dependent kinase II, affect the trafficking and gating of Nav1.5 (39). Eleven "basal" phosphorylation sites have been identified in Nav1.5 purified from adult mouse ventricular tissue (40). It remains to be determined whether PI3K signaling alters the modification of these or other phosphorylation sites to regulate I_{NaP}. The ability of Akti treatment to increase I_{NaP} suggests that Akt might phosphorylate Nav1.5 to regulate the current. It is interesting that the increase in I_{NaP} observed in the presence of Akti was less than that observed in myocytes from diabetic mice (Fig. 2) or from mice lacking the p110α isoform of PI3K (8), suggesting that other kinases downstream of PI3K might also be involved in regulating the current. A recent study examined transgenic mice with cardiac-specific expression of a constitutively active form of serum- and glucocorticoid-regulated kinase-1 (CA-SGK1), a downstream effector of PI3K that is structurally related to Akt. Unlike our results and those using transgenic mice expressing constitutively active p110α (32), cardiac myocytes from CA-SGK1 mice exhibited APD prolongation and an increase in I_{NaP} (41). The apparent discrepancy between these results could be due to differential regulation of I_{NaP} and other currents that define the cardiac action potential by different protein kinases downstream of PI3K.

In conclusion, we have shown that decreased PI3K signaling in the diabetic mouse heart leads to an increase in I_{NaP}, which plays a major role in provoking QT prolongation. These findings are consistent with our study showing that cardiac-specific ablation of the PI3K catalytic subunit p110α resulted in elevated I_{NaP} and QT prolongation in mice, and that pharmacological inhibition of PI3K signaling in canine myocytes led to APD prolongation and alterations in multiple currents, with the increase in I_{NaP} and decrease in I_{Kr} contributing the most to APD prolongation (8). Based on these results, we predict that diabetic patients have multiple cardiac ion current abnormalities that predispose them to long QT syndrome and that decreased PI3K signaling due to insulin resistance is a mechanistic explanation for QT prolongation in this patient population.

ACKNOWLEDGMENTS

This work was funded by NIH grants DK-62722 (R.Z.L.), HL-67101 (I.S.C.), and HL-94410 (I.S.C.) and a Veterans Affairs Merit Award (R.Z.L.).

No potential conflicts of interest relevant to this article were reported.

Z.L., Y.-P.J., C.-Y.C.W., L.M.B., and S.L. performed the experiments, analyzed data, and wrote the manuscript. E.S.C. generated the CAp110α adenovirus. M.R.R. contributed to the discussion, analyzed data, and wrote the manuscript. I.S.C. and R.Z.L. supervised the study, analyzed data, provided funding, and wrote the manuscript. R.Z.L. is the guarantor of this work and, as such, had full access to all the data in the study and takes responsibility for the integrity of the data and the accuracy of the data analysis.

REFERENCES

1. Rydén L, Standl E, Bartnik M, et al.; Task Force on Diabetes and Cardiovascular Diseases of the European Society of Cardiology (ESC); European Association for the Study of Diabetes (EASD). Guidelines on diabetes, prediabetes, and cardiovascular diseases: executive summary. Eur Heart J 2007;28:88–136
2. Hedley PL, Jørgensen P, Schlamowitz S, et al. The genetic basis of long QT and short QT syndromes: a mutation update. Hum Mutat 2009;30:1486–1511
3. Veglio M, Borra M, Stevens LK, Fuller JH, Perin PC; The EURODIAB IDDM Complication Study Group. The relation between QTc interval prolongation and diabetic complications. Diabetologia 1999;42:68–75
4. Veglio M, Bruno G, Borra M, et al. Prevalence of increased QT interval duration and dispersion in type 2 diabetic patients and its relationship with coronary heart disease: a population-based cohort. J Intern Med 2002;251:317–324
5. Okin PM, Devereux RB, Lee ET, Galloway JM, Howard BV; Strong Heart Study. Electrocardiographic repolarization complexity and abnormality predict all-cause and cardiovascular mortality in diabetes: the strong heart study. Diabetes 2004;53:434–440
6. Rossing P, Breum L, Major-Pedersen A, et al. Prolonged QTc interval predicts mortality in patients with type 1 diabetes mellitus. Diabet Med 2001;18:199–205
7. Veglio M, Sivieri R, Chinaglia A, Scaglione L, Cavallo-Perin P. QT interval prolongation and mortality in type 1 diabetic patients: a 5-year cohort prospective study. Neuropathy Study Group of the Italian Society of the Study of Diabetes, Piemonte Affiliate. Diabetes Care 2000;23:1381–1383
8. Z. Lu, C.Y. Wu, Y.P. Jiang, et al. Suppression of phosphoinositide 3-kinase signaling and alteration of multiple ion currents in drug-induced long QT syndrome. Sci Transl Med 2012;4:131ra150
9. Wang L, Feng ZP, Kondo CS, Sheldon RS, Duff HJ. Developmental changes in the delayed rectifier K+ channels in mouse heart. Circ Res 1996;79:79–85
10. Hoshino S, Omatsu-Kanbe M, Nakagawa M, Matsuura H. Postnatal developmental decline in IK1 in mouse ventricular myocytes isolated by the Langendorff perfusion method: comparison with the chunk method. Pflugers Arch 2012;463:649–668
11. Nuyens D, Stengl M, Dugarmaa S, et al. Abrupt rate accelerations or premature beats cause life-threatening arrhythmias in mice with long-QT3 syndrome. Nat Med 2001;7:1021–1027
12. Salama G, London B. Mouse models of long QT syndrome. J Physiol 2007;578:43–53
13. He TC, Zhou S, da Costa LT, Yu J, Kinzler KW, Vogelstein B. A simplified system for generating recombinant adenoviruses. Proc Natl Acad Sci USA 1998;95:2509–2514
14. Ballou LM, Tian PY, Lin HY, Jiang YP, Lin RZ. Dual regulation of glycogen synthase kinase-3β by the α_{1A}-adrenergic receptor. J Biol Chem 2001;276:40910–40916
15. Mitchell GF, Jeron A, Koren G. Measurement of heart rate and Q-T interval in the conscious mouse. Am J Physiol 1998;274:H747–H751
16. Ballou LM, Selinger ES, Choi JY, Drueckhammer DG, Lin RZ. Inhibition of mammalian target of rapamycin signaling by 2-(morpholin-1-yl)pyrimido[2,1-α]isoquinolin-4-one. J Biol Chem 2007;282:24463–24470
17. Ballou LM, Cross ME, Huang S, McReynolds EM, Zhang BX, Lin RZ. Differential regulation of the phosphatidylinositol 3-kinase/Akt and p70 S6 kinase pathways by the α_{1A}-adrenergic receptor in rat-1 fibroblasts. J Biol Chem 2000;275:4803–4809
18. Lu Z, Jiang YP, Xu XH, Ballou LM, Cohen IS, Lin RZ. Decreased L-type Ca2+ current in cardiac myocytes of type 1 diabetic Akita mice due to reduced phosphatidylinositol 3-kinase signaling. Diabetes 2007;56:2780–2789
19. Magyar J, Rusznák Z, Szentesi P, Szûcs G, Kovács L. Action potentials and potassium currents in rat ventricular muscle during experimental diabetes. J Mol Cell Cardiol 1992;24:841–853
20. Jourdon P, Feuvray D. Calcium and potassium currents in ventricular myocytes isolated from diabetic rats. J Physiol 1993;470:411–429
21. Wang DW, Kiyosue T, Shigematsu S, Arita M. Abnormalities of K+ and Ca2+ currents in ventricular myocytes from rats with chronic diabetes. Am J Physiol 1995;269:H1288–H1296
22. Shimoni Y. Inhibition of the formation or action of angiotensin II reverses attenuated K+ currents in type 1 and type 2 diabetes. J Physiol 2001;537:83–92
23. Pereira L, Matthes J, Schuster I, et al. Mechanisms of [Ca2+]i transient decrease in cardiomyopathy of db/db type 2 diabetic mice. Diabetes 2006;55:608–615
24. Shimoni Y, Chuang M, Abel ED, Severson DL. Gender-dependent attenuation of cardiac potassium currents in type 2 diabetic db/db mice. J Physiol 2004;555:345–354
25. Lu Z, Ballou LM, Jiang YP, Cohen IS, Lin RZ. Restoration of defective L-type Ca2+ current in cardiac myocytes of type 2 diabetic db/db mice by Akt and PKC-ι. J Cardiovasc Pharmacol 2011;58:439–445
26. Zhang Y, Xiao J, Lin H, et al. Ionic mechanisms underlying abnormal QT prolongation and the associated arrhythmias in diabetic rabbits: a role of rapid delayed rectifier K+ current. Cell Physiol Biochem 2007;19:225–238
27. Zhang Y, Xiao J, Wang H, et al. Restoring depressed HERG K+ channel function as a mechanism for insulin treatment of abnormal QT prolongation and associated arrhythmias in diabetic rabbits. Am J Physiol Heart Circ Physiol 2006;291:H1446–H1455
28. Lengyel C, Virág L, Bíró T, et al. Diabetes mellitus attenuates the repolarization reserve in mammalian heart. Cardiovasc Res 2007;73:512–520
29. Tian XL, Yong SL, Wan X, et al. Mechanisms by which SCN5A mutation N1325S causes cardiac arrhythmias and sudden death in vivo. Cardiovasc Res 2004;61:256–267
30. Charpentier F, Bourgé A, Mérot J. Mouse models of SCN5A-related cardiac arrhythmias. Prog Biophys Mol Biol 2008;98:230–237
31. Schwartz PJ, Priori SG, Locati EH, et al. Long QT syndrome patients with mutations of the SCN5A and HERG genes have differential responses to Na+ channel blockade and to increases in heart rate. Implications for gene-specific therapy. Circulation 1995;92:3381–3386
32. Yang KC, Foeger NC, Marionneau C, Jay PY, McMullen JR, Nerbonne JM. Homeostatic regulation of electrical excitability in physiological cardiac hypertrophy. J Physiol 2010;588:5015–5032
33. Cook SA, Varela-Carver A, Mongillo M, et al. Abnormal myocardial insulin signalling in type 2 diabetes and left-ventricular dysfunction. Eur Heart J 2010;31:100–111
34. Wang B, Raedschelders K, Shravah J, et al. Differences in myocardial PTEN expression and Akt signalling in type 2 diabetic and nondiabetic

patients undergoing coronary bypass surgery. Clin Endocrinol (Oxf) 2011; 74:705–713
35. Carroll R, Carley AN, Dyck JR, Severson DL. Metabolic effects of insulin on cardiomyocytes from control and diabetic db/db mouse hearts. Am J Physiol Endocrinol Metab 2005;288:E900–E906
36. Hafstad AD, Solevåg GH, Severson DL, Larsen TS, Aasum E. Perfused hearts from type 2 diabetic (db/db) mice show metabolic responsiveness to insulin. Am J Physiol Heart Circ Physiol 2006;290:H1763–H1769
37. Mazumder PK, O'Neill BT, Roberts MW, et al. Impaired cardiac efficiency and increased fatty acid oxidation in insulin-resistant ob/ob mouse hearts. Diabetes 2004;53:2366–2374
38. Lee J, Xu Y, Lu L, et al. Multiple abnormalities of myocardial insulin signaling in a porcine model of diet-induced obesity. Am J Physiol Heart Circ Physiol 2010;298:H310–H319
39. Rook MB, Evers MM, Vos MA, Bierhuizen MF. Biology of cardiac sodium channel Nav1.5 expression. Cardiovasc Res 2012;93:12–23
40. Marionneau C, Lichti CF, Lindenbaum P, et al. Mass spectrometry-based identification of native cardiac Nav1.5 channel α subunit phosphorylation sites. J Proteome Res 2012;11:5994–6007
41. Das S, Aiba T, Rosenberg M, et al. Pathological role of serum- and glucocorticoid-regulated kinase 1 in adverse ventricular remodeling. Circulation 2012;126:2208–2219